Escherichia coli membrane microdomain SPFH protein HflC interacts with YajC and contributes to aminoglycoside and oxidative stress tolerance

Aimee K. WESSEL[1†], Yutaka YOSHII[1†], Alexander REDER[2], Rym BOUDJEMAA[3], Magdalena SZCZESNA[1,6], Jean-Michel BETTON[4], Joaquin BERNAL-BAYARD[1,7], Christophe BELOIN[1], Daniel LOPEZ[5], Uwe VÖLKER[2], Jean-Marc GHIGO[1*]

[1] *Institut Pasteur, Université de Paris-Cité, CNRS UMR6047, Genetics of Biofilms Laboratory F-75015 Paris, France.*

[2] *Department of Functional Genomics, Interfaculty Institute for Genetics and Functional Genomics, University Medicine Greifswald, 17487 Greifswald, Germany.*

3 Abbelight, 191 avenue Aristide Briand, 94230 Cachan

[4] *Institut Pasteur, Université de Paris-Cité,, UMR UMR6047, Stress adaptation and metabolism in enterobacteria 75015 Paris, France.*

[5] *Universidad Autonoma de Madrid, Centro Nacional de Biotecnologia, Campus de Cantoblanco, Calle Darwin 3, 28049 Madrid, España*

[6] *MRC Centre for Molecular Bacteriology and Infection, Imperial College London, Armstrong Road, London SW7 2AZ, UK*

[7] *Departamento de Genética, Facultad de Biología, Universidad de Sevilla, Apartado 1095, 41080 Sevilla, Spain*

† AW and YY equally contributed to this work.

[*]**Corresponding author:** Jean-Marc Ghigo (jean-marc.ghigo@pasteur.fr)

Short Title: *E. coli* SPFH lipid raft proteins contribute to tobramycin and paraquat tolerance

Keywords

Lipid raft; membrane micro-domains; SPFH; Flotilin; Stress tolerance; *Escherichia coli*

ABSTRACT

Eukaryotic cells segregate many membrane-dependent functions into membrane microdomains also known as lipid rafts. These domains are enriched in polyisoprenoid lipids and in scaffolding proteins belonging to the Stomatin, Prohibitin, Flotillin, and HflK/C (SPFH) protein superfamily, which are also found in prokaryotes. Whereas Gram-positive bacteria were also shown to possess functional membrane microdomains (FMMs) structurally and functionally similar to eukaryotic lipid rafts, little is still known about Gram-negative bacteria FMMs. *Escherichia coli* K12 possesses 4 SPFH proteins, YqiK, QmcA, HflK, and HflC, previously shown to localize in discrete polar or lateral inner-membrane locations, raising the possibility that *E. coli* SPFH proteins could contribute to the assembly of inner-membrane FMMs regulating cellular processes.

Here we studied the determinants of the native, chromosomal QmcA and HflC cell localization using a domain swap analysis and fluorescent and super-resolution microscopy. We showed that full QmcA and HflC protein is required for achieving their native inner-membrane localization and that impairing the synthesis of cardiolipin and isoprenoid lipids known to associate with FMMs alters QmcA and HflC localization pattern. Finally, using Biolog phenotypic arrays, we showed that a mutant lacking all SPFH genes displayed increased sensitivity to aminoglycosides and oxidative stress. This phenotype is exclusively due to the absence of HflKC and a cross-linking and mass spectrometry analysis showed that YajC, a SecDF translocon accessory protein, interacts with HflC and also contributes to *E. coli* stress tolerance. Our study therefore provides insights into the function and interactions associated with SPFH proteins in *E. coli* FMMs.

67 **IMPORTANCE**

68

69 Eukaryotic cells segregate many cellular processes in cholesterol-rich functional
70 membrane micro-domain also called lipid rafts, which contain proteins of the Stomatin,
71 Prohibitin, Flotillin, and HflK/C (SPFH) superfamily. Whereas SPFH proteins are also
72 present in bacteria, they were mostly studied in Gram-positive bacteria and less is known
73 on the function of SPFH proteins in Gram-negative bacteria. Here, we showed that the
74 cell localization of the *E. coli* SPFH proteins QmcA and HflKC is altered in absence of
75 cardiolipin and isoprenoid lipid synthesis, suggesting that these lipids could contribute to
76 *E. coli* membrane microdomain assembly. Using a broad phenotypic analysis and cross-
77 linking coupled with spectrometry approaches, we identified that YajC, a SecDF-YajC
78 translocon accessory protein, interacts with HflC and that both proteins contribute to *E.*
79 *coli* tolerance to aminoglycosides and oxidative stress. Our study, therefore, provides new
80 insights into the cellular processes associated with SPFH proteins in *E. coli* functional
81 membrane microdomains.

82

83 **INTRODUCTION**

84

85 In addition to separating the intracellular content of cells from the environment, lipid
86 bilayer membranes also contribute to specialized functions, including cross-membrane
87 transport, enzymatic activity, signaling as well as anchoring of cytoskeletal and
88 extracellular structures (1, 2). In eukaryotes, these membrane-dependent functions are
89 spatially and temporally regulated by membrane microdomains called lipid rafts (3-5),
90 broadly defined as cholesterol- and sphingolipid-enriched membrane regions formed
91 upon lipid-lipid, lipid-protein and protein-protein interactions that compartmentalize
92 membrane cellular processes (5-7). The Stomatin/Prohibitin/Flotillin/HflK/C (or SPFH)
93 family of membrane proteins has been shown to localize in eukaryotic lipid rafts and to
94 recruit and provide a stabilizing scaffold to other lipid raft-associated proteins (8-13).
95 Although sphingolipids and cholesterol are absent from most prokaryotes (14), the Gram-
96 positive bacteria *Bacillus subtilis* and *Staphylococcus aureus* can also compartmentalize
97 cellular processes in functional membrane microdomains (FMMs) (14-16). Analogous to
98 eukaryote lipid rafts, bacterial FMMs display a distinct lipidic composition and are
99 enriched in farnesol, hopanoids and other polyisoprenoid lipids (14, 16, 17). They also
100 contain SPFH proteins, including flotillins, and a pool of proteins involved in diverse
101 cellular processes (14, 16). In *B. subtilis*, flotillins FloT and FloA colocalize in membrane
102 foci and contribute to the assembly of membrane protein complexes (18-21). Lack of
103 flotillins impairs biofilm formation, sporulation, protease secretion, motility, and natural
104 competence, indicating that the formation of FMMs also plays critical cellular roles in *B.*
105 *subtilis* (15, 18, 22-25).
106 SPFH proteins are also found in Gram-negative bacteria and *Escherichia coli* K12
107 possesses four genes, *yqiK*, *qmcA*, *hflK*, and *hflC*, which encode proteins with a SPFH
108 domain and a N-terminal transmembrane segment (26). QmcA and YqiK are predicted to
109 face the cytoplasmic compartment, while HflK and HflC are predicted to be exposed in
110 the periplasm, forming the HflKC complex negatively regulating the protease activity of
111 FtsH against membrane proteins (27-30). HflC and QmcA are detected in *E. coli*
112 membrane fractions resistant to solubilization by non-ionic detergents (detergent-resistant
113 membranes or DRM) that are often used as - debatable - proxies for FMMs (31-34).
114 Moreover, fluorescent microscopy showed that *E. coli* SPFH proteins HflC and QmcA

115 are localized in discrete polar or lateral membrane foci (35). This raised the possibility
116 that *E. coli* SPFH proteins could localize in inner-membrane FMMs and regulate
117 important cellular processes (36). However, apart from the functional and structural
118 description of HflKC as a regulator of the FtsH membrane protease (27, 30, 37) and a
119 recent study suggesting that YqiK is involved in cell motility and resistance to ampicillin
120 (38), the functions of FMM in *E. coli* and other Gram negative bacteria are still poorly
121 understood.
122 In this study, we used fluorescent and super resolution microscopy to perform a detailed
123 analysis of QmcA and HflC membrane localization signals. We then showed that integrity
124 of QmcA and HflC protein domains is required for their inner membrane localization,
125 and that the lack of cardiolipin and isoprenoid lipids known to associate with FMMs alters
126 their localization. Moreover, using single and multiple SPFH gene mutants, we showed
127 that the absence of HflKC increases sensitivity to aminoglycosides and oxidative stress.
128 Finally, cross-linking and mass spectrometry analysis allowed us to identify YajC, a
129 protein of unknown function and an accessory component of the SecDF-YajC translocon,
130 as a new partner that interacts and colocalizes with HflC at the cell pole and contributes
131 to stress tolerance Our study therefore provides new insights into the function and
132 interactions associated with *E. coli* SPFH proteins.
133
134

135 **RESULTS**
136
137 **Chromosomal *E. coli* SPFH fluorescent fusion proteins show distinct localization**
138 **patterns.**
139
140 To investigate the determinant of cell localization of *E. coli* SPFH proteins, we first
141 tagged YqiK and QmcA, which C-termini are predicted to be in the cytoplasm (29), with
142 a C-terminal monomeric super folder green fluorescent protein (msfGFP). We then
143 tagged HflC and HflK, which C-termini are predicted to be in the periplasm (29), with
144 the C-terminal red fluorescent protein mCherry. All these fusions were expressed under
145 their own promoter from their native chromosomal location (Sup. Fig. S1).
146 Epifluorescence and super-resolution microscopy confirmed the previously reported
147 polar localization of HflK and HflC (35) (Fig. 1 and Sup. Fig. S2), with 94% and 91%
148 polar localization pattern for HflC-mCherry and HflK-mCherry, respectively (n=150). By
149 contrast, C-terminally tagged QmcA-GFP localized exclusively as punctate distributed
150 throughout the cell body, with 96% of the cells harboring 5 foci or more (n=150) (Fig.
151 1CD). However, we could not detect YqiK-GFP, possibly due to its low native
152 chromosomal expression level. We then used anti-GFP or mCherry antibodies to perform
153 immunodetection on cytoplasmic as well as inner and outer membrane fractions of *E. coli*
154 strains expressing either HflC-mCherry or QmcA-GFP. In agreement with previous
155 results (29, 36), both fusion proteins were detected in the inner membrane fraction (Fig.
156 2).
157
158 **Domain swap analysis shows that protein integrity is essential for QmcA-GFP and**
159 **HflC-mCherry localization.**
160
161 To identify HflC and QmcA membrane localization signals, we constructed multiple
162 fluorescently tagged truncated version of both proteins. We tagged with msfGFP a QmcA
163 protein reduced to its transmembrane region and SPFH domain (TM^{QmcA}-$SPFH^{QmcA}$-
164 GFP) and, separately, one reduced to the QmcA transmembrane region only (TM^{QmcA}-
165 GFP) (Fig. 3A). To test the role of the QmcA transmembrane region, we also swapped
166 TM^{QmcA} in the three constructions by the single-spanning TM domain of the phage coat
167 protein Pf3 (TM^{Pf3}), which orients subsequent amino acids to the cytosol (38) (Fig. 3A).
168 Similarly, in addition to the full length HflC-mCherry, we tagged with mCherry the HflC
169 transmembrane region and SPFH domain (TM^{HflC}-$SPFH^{HflC}$-mCherry) and, separately,

170 only its TM region (TM^{HflC}-mCherry) (Fig. 3B). We also swapped the HflC TM region
171 with the single-spanning TM region of colistin M immunity protein (TM^{Cmi}), which
172 orients subsequent amino acids to the periplasm (39) (Fig. 3B). Epifluorescence
173 microscopy of HflC and QmcA derivative fusions showed that in addition to full-length
174 constructs only full-length constructs with swapped TM (TM^{Pf3}-QmcA-GFP and TM^{Cmi}-
175 HflC-mCherry) displayed significant punctated foci or polar localization, respectively
176 (Fig. 3AB), although at reduced frequency compared to native QmcA-GFP and HflC-
177 mCherry. Finally, we prepared inner and outer membrane fractions of *E. coli* strains
178 expressing each QmcA and HflC derivative and we observed that all these constructs
179 were still mainly located in the inner membrane fraction. This indicates that, while we
180 observed that QmcA-GFP and HflC-mChery derivatives exhibit altered cell localization,
181 they do not exhibit significant mis-localization and remain located in the inner membrane
182 (Sup. Fig. S3). These results therefore indicated that specific QmcA and HflC localization
183 requires the combination of a transmembrane and full cytoplasmic (QmcA) or
184 periplasmic (HflC) domain.
185
186 **Lack of cardiolipin and isoprenoid lipid synthesis alters the cell localization of**
187 **QmcA and HflC.**
188
189 FMMs were previously shown to be enriched with negatively charged cardiolipins and
190 isoprenoids, which promote the localization of polar proteins and modulation of
191 membrane lipid fluidity (15, 22, 39-42). We first tested whether alteration of cardiolipin
192 synthesis could cause mis-localization of *E. coli* SPFH proteins QmcA or HflKC in a
193 mutant lacking the major cardiolipin synthases *clsABC* (43). Whereas epifluorescence
194 microscopy analysis did not show clear alteration of QmcA-GFP punctate localization
195 patterns in a *clsABC* mutant, single-molecule 2 and 3D super-resolution microscopy
196 analysis showed a 3 to 10-fold reduction of the number of QmcA-GFP punctates
197 compared to WT (Fig. 4A and Sup. Fig. S4). Super-resolution microscopy analysis of
198 HflC-mCherry localization showed a drastic loss of polar localization pattern (Fig. 4B
199 and Supp. Fig. S4). We then used an *idi* mutant unable to synthesize isoprenoid lipids due
200 to the lack of isomerization of isopentenyl diphosphate (IPP) into dimethylallyl
201 diphosphate (DMAPP) (44). We observed that, whereas QmcA-GFP punctate
202 localization is not affected, HflC-mCherry polar localization was reduced in the Δ*idi*

203 mutant (Fig. 4A and Sup. Fig. S4). These results demonstrate that the modulation of
204 membrane lipid fluidity alters FMM protein localization in *E. coli*.
205
206 **Phenotypic analysis of *E. coli* SPFH mutant shows that only absence of HflKC**
207 **increases *E. coli* sensitivity to aminoglycosides and oxidative stress.**
208
209 To identify potential phenotypes and functions associated with the *E. coli* SPFH proteins
210 YqiK, QmcA, HflK and HflC, we introduced single and multiple deletions of the
211 corresponding SPFH genes and observed that neither single mutants nor the quadruple
212 Δ*hflK,* Δ*hflC,* Δ*qmcA*, and Δ*yqiK* (hereafter referred to Δ*SPFH* mutant) displayed any
213 significant growth defects in rich or minimal media (Fig. 5A and Sup. Fig. S5A).
214 Considering the role of SPFH proteins in activation of inner-membrane kinases involved
215 in *B. subtilis* biofilm formation (15), we tested adhesion and biofilm capacity of WT and
216 ΔSPFH strains but could not detect any significant differences between these two strains.
217 We then used Biolog^{TM} phenotypic microarrays to perform a large-scale phenotypic assay
218 comparing an *E. coli* WT and Δ*SPFH* mutant, (Sup. Table S1). This analysis revealed
219 that the Δ*SPFH* mutant is metabolically less active when grown in the presence of various
220 aminoglycosides (tobramycin, capreomycin, sisomicin and paromomycin) or when
221 exposed to paraquat (Fig. 5B and Sup. Fig. S5BC). Consistently, the minimal inhibitory
222 concentration (MIC) for tobramycin of the Δ*SPFH* mutant was 3-fold lower than that of
223 the WT MIC (Fig.5C) and the sensitivity of the Δ*SPFH* mutant to paraquat was increased
224 compared to the WT (Fig. 5D and Sup. Fig. S5D). Test of individual SPFH-gene mutants
225 for their sensitivity to tobramycin and paraquat showed that the HflKC complex is the
226 sole responsible for both phenotypes, as both single *hflK* and *hflC* or a double *hflKC*
227 mutants displayed increased sensitivity to tobramycin and oxidative stress (Fig. 5CD and
228 Sup. Fig. S5E). This phenotype could be complemented upon introduction of a plasmid
229 expressing *hflKC* genes in the double *hflKC* mutant (Sup. Fig. S6A). Finally, whereas an
230 Δ*idi* mutant showed no significant difference compared to the WT, the MIC for
231 tobramycin and paraquat of a Δ*clsABC* mutant was reduced by 2 to 3-fold, consistent with
232 the impact of a *cls* mutation on HflC localization (Fig. 4BD and Fig.5CD).
233
234

235 **YajC interacts and colocalizes with HflC and contributes to tobramycin and**
236 **paraquat tolerance**
237
238 Considering the scaffolding role of HflKC, we hypothesized that proteins interacting with
239 HflKC in FMMs could also contribute to tolerance to aminoglycosides and paraquat. We
240 first tested AcrA, the efflux pump involved in the transport of a wide range of substrates
241 including aminoglycosides (45) and YidC, an essential inner membrane protein required
242 for proper insertion of integral inner membrane proteins (46). Both proteins were indeed
243 previously identified in *E. coli* inner-membrane DRM fractions often biochemically
244 associated with FMM and shown to display HflC-type pattern of polar localization when
245 fused to fluorescent proteins and expressed from plasmids (35, 47). However, when
246 expressed from their native chromosomal context, we could not detect any distinct AcrA-
247 GFP nor YidC-GFP localization nor any significant co-localisation with HflC in
248 exponential or stationary phase conditions (Sup. Fig. S7). Moreover, an *acrA* deletion did
249 not alter *E. coli* MIC profile to tobramycin and paraquat as much as a Δ*hflC* mutant
250 (Fig.5CD). To define additional interaction partners of HflC, we decided to use a cross-
251 linking approach followed by affinity chromatography and mass spectrometric
252 identification of interacting proteins. To this end, we created a translation fusion of HflC
253 with a C-terminal double Tag consisting of a TwinStrep-Tag followed by a poly-
254 Histidine-Tag (hereafter referred to *HflC-tag* fusion) at the native chromosomal locus.
255 Expression of the fusion from the *hflC* promoter ensured native expression levels and
256 minimized detection of false-positive interaction candidates due to non-physiological
257 protein levels. Proteins were cross-linked covalently by formaldehyde treatment in
258 quadruplicates in exponentially growing and stationary phase cells. Complexes of HflC
259 were purified with StepTactinXT magnetic beads from both conditions and 11 or 17
260 possible direct interaction partners were identified by mass spectrometry in exponentially
261 growing or stationary phase *E. coli*, respectively (Sup. Fig. S8 and Sup. Table S2 and S3).
262 In both tested conditions, we not only identified as potential interaction partners the two
263 well-known HflC interaction partners HflK and FtsH (27), but also YajC, a Sec translocon
264 accessory subunit membrane protein of unknown function, and two periplasmic proteins,
265 the thiol-reductase chaperone DsbG and the cell division coordinator of peptidoglycan
266 synthesis CpoB (Sup. Fig. S8 and Sup Table S3).

267 To validate these 3 new HflC partners, we performed localization experiments for all
268 three candidate proteins. Whereas DsbG-GFP and CpoB-GFP fusions did not display a
269 HflC-type pattern of polar localization. (Sup. Fig. S7), we could show that YajC-GFP co-
270 localized with HflC-mCherry at cell poles (93%; n=150) (Fig 6A). Moreover, a Δ*yajC*
271 mutant displayed an increased sensitivity to tobramycin and paraquat (Fig 6 BC), which
272 could be partially reverted upon complementation with a plasmid expressing *yajC* (Sup.
273 Fig. S6AB and S8). Nevertheless, YajC-GFP polar localization was not altered in
274 Δ*clsABC,* Δ*idi,* and Δ*hflC* mutants (Sup. Fig. S9), suggesting that YajC function or its
275 localization are not strictly dependent on the presence of HflC. Taken together, these
276 results indicate that the HflKC SPFH protein complex interacts with YajC and contributes
277 to oxidative and antibiotic stress resistance.

278 **DISCUSSION**
279

280 SPFH-domain proteins have been identified in most organisms (16, 48). However,
281 whereas SPFH-domain proteins have been extensively studied in Eukaryotes (3, 5, 49),
282 prokaryotic SPFH proteins and proteins associated with functional membrane
283 microdomains (FMMs) are much less understood. This is particularly the case for Gram-
284 negative bacteria, in which potential FMMs functions are mostly inferred from studies
285 performed in *B. subtilis* and *S. aureus*.
286

287 In this study, we investigated the functions and the localization determinants of *E. coli*
288 SPFH proteins. We first used a domain deletion and replacement approach and showed
289 that, although most of the tested domain replacement variants correctly localized to the
290 inner membrane, they failed to display WT protein localization patterns. This indicates
291 that inner-membrane localization alone is not sufficient for correct subcellular
292 distribution of HflC and QmcA, whose localization signals might rely on multiple
293 addressing sequences spread throughout the entirety of each protein.
294

295 The very different localization patterns of QmcA and HflKC SPFH proteins suggests that
296 they could each be part of different FMMs, potentially using different localization signals
297 and involved in different cellular processes. The punctate localization pattern displayed
298 by QmcA-GFP fusion was also observed in the case of *E. coli* YqiK expressed from
299 plasmid and of the flotillin homologues in *B. subtilis*, *S. aureus*, and *B. anthracis* flotillin
300 homologues (15, 16, 50-52). Interestingly, *B. subtilis* and *S. aureus* flotillin genes are
301 found associated with a gene encoding an NfeD protein, which that could contribute to
302 protein-protein interactions within flotillin assemblies (53, 54). Consistently, like *yqiK*,
303 *E. coli qmcA* gene is located upstream of the NfeD-like *ybbJ* gene. This further supports
304 the notion that QmcA, like YqiK, can be considered as an *E. coli* flotillin. By contrast,
305 the *hflKC* transcription unit lacks a downstream *nfeD* gene, suggesting that HflKC may
306 not be a *bona fide* flotillin. However, while QmcA and YqiK have opposite orientation to
307 HflK and HflC, they are structurally similar proteins and the four *E. coli* SPFH proteins
308 could therefore share some degrees of functionalities. The topological similarity between
309 HflK and HflC might contribute to HflKC complex formation and its interaction with

310 FtsH protease, resulting in a large periplasmic FtsH-HflKC complex localized at the cell
311 pole (27, 28, 55-57).
312 The strong negative impact of QmcA or HflC transmembrane (TM) domain replacement
313 suggests that QmcA or HflC TM domains could recognize specific membrane lipid
314 composition facilitating the recruitment of SPFH proteins at their proper cellular
315 membrane localization. Along with phosphatidylethanolamine and phosphatidylglycerol,
316 cardiolipins are the primary constituent components of *E. coli* membranes that
317 concentrate into cell poles and dividing septum (58-61). It was indeed observed that the
318 composition of *E. coli* membrane lipid at cell poles is altered in a *clsABC* cardiolipin
319 deficient mutant, compensated by an increased amount of phosphatidylglycerol (62).
320 Several studies reported that cardiolipin-enriched composition in membranes at cell poles
321 influences both the localization and activity of inner membrane proteins such as
322 respiratory chain protein complexes and the osmosensory transporter ProP (39, 40, 63-
323 65). In this study, we showed that, similarly to ProP, HflC and QmcA localization patterns
324 are drastically affected in a *ΔclsABC* mutant, suggesting that *E. coli* FMMs are
325 cardiolipin-rich microdomains, in which HflKC and QmcA complexes could act as a
326 scaffold for FMMs cargo proteins.
327
328 Isoprenoid lipds such as farnesol, carotenoids, and hopanoids are constituents of bacterial
329 FMMs and interact with SPFH proteins and FMM-associated proteins (14). Blocking the
330 *S. aureus* carotenoid synthetic pathway by zaragozic acid leads to flotillin mis-
331 localization (15). Moreover, inactivation of farnesol synthesis in a *B. subtilis yisP* mutant,
332 which is defective for production of farnesol, impairs focal localization of the FMM-
333 associated sensor kinase KinC (15). We showed here that in *E. coli*, interfering with the
334 *idi* isoprenoid biosynthesis pathway also strongly alters the localization of HflC. This
335 further documents that isoprenoid lipids contribute to the formation or integrity of FMMs,
336 possibly by altering isoprenoid-dependent membrane rigidity, as shown in *S. aureus* and
337 *B. subtilis* FMMs (14, 66).
338 Our phenotypic investigation of the function of *E. coli* SPFH proteins showed that a
339 ΔSPFH mutant displays increased susceptibility to oxidative stress and aminoglycosides,
340 and this sensitivity was due to the absence of HflKC. The HflKC complex was previously
341 shown to modulate the quality control proteolytic activity of FtsH by regulating the access

342 of misfolded membrane protein products to FtsH (27, 28, 67). *E. coli* Δ*hflK* and Δ*hflC*
343 mutant strains were also shown to accumulate increased amounts of hydroxyl radical,
344 suggesting that HflK and HflC could influence tolerance to aminoglycosides and
345 oxidative stress by suppressing excessive hydroxyl radical production. Alternatively,
346 HflK and HflC could contribute to tobramycin resistance via FtsH-dependent proteolytic
347 activity (68) or favoring FMM formation and the assembly of membrane proteins and
348 lipids, such as cardiolipin, involved in the transport and movement of aminoglycosides
349 within cells and cell membranes. Consistently, several proteins associated with
350 aminoglycosides transport were actually detected in *E. coli* DRM fractions, including
351 proteins involved in LPS transport (LptC, G and F), phospholipid transport (MlaD, MlaE,
352 YebT and PqiB) and several components of the AcrAB-TolC efflux pump (35),
353 suggesting that deletion of *hflK* or *hflC* could reduce the activity of these proteins in
354 FMMs and enhance entry of aminoglycosides. Whereas the susceptibility to
355 aminoglycosides indeed partly relies on the AcrAB-TolC efflux pump (45, 69-71), we
356 found that lack of the AcrA only moderately decreases the MIC to tobramycin, compared
357 to a *hflKC* mutation.
358 The use of a cross-linking approach followed by mass spectrometric analysis allowed us
359 to identify YajC as a new HflC interacting partner. YajC is described as an unknown
360 function accessory membrane protein contributing to the association between SecA and
361 SecYEG translocon (72-74). Consistently with its association with HflC, the deletion of
362 *yajC* reduced sensitivity to tobramycin and paraquat, however to a greater extent than in
363 a Δ*SPFH* or Δ*hflKC* mutants, suggesting that lack of YajC could have a muti-factorial
364 effect on *E. coli* antibiotic and oxidative stress resistance. Interestingly, a pump
365 component, AcrB, was shown to co-crystalize with YajC (75). Hence, HflC could play a
366 scaffolding role, facilitating YajC interactions with the SecDF or AcrAB-TolC protein
367 complexes. However, the polar localization of YajC was not altered by the absence of
368 HflC, nor in a Δ*clsABC* mutant, indicating that YajC is not strictly FMM-dependent. YajC
369 could therefore itself be a scaffolding protein and we speculate that YajC and the HflKC-
370 FtsH complex could be interacting only when independently localizing at cell poles.
371 There, the lack of cardiolipin could only lead to a partial defect of HflC-YajC interactions,
372 consistent with the observed slight increased susceptibility of a Δ*clsABC* mutant for
373 tobramycin and paraquat compared to a wild type *E. coli*.

In conclusion, the present study provides new insights into the functions of *E. coli* SPFH proteins and some of their interacting partners and further experiments will be needed to fully uncover the roles played by this intriguing family of membrane proteins in Gram-negative bacteria.

381 **MATERIALS & METHODS**

382

383 **Bacterial strains and growth conditions**

384 Bacterial strains and plasmids used in this study are described in Sup. Table S4, and
385 further explained in Sup. Fig. S1 and Figure 3. Unless stated otherwise, all experiments
386 were performed in lysogeny broth (LB) or M63B1 minimal medium supplemented with
387 0.4% glucose (M63B1.G) at 37 °C. Antibiotics were used as follows: kanamycin (50
388 µg/mL); chloramphenicol (25 µg/mL); ampicillin (100 µg/mL); and zeocin (50 µg/mL).
389 All compounds were purchased from Sigma-Aldrich (St Louis, MO, USA) except for
390 Zeocin (InvivoGen, Santa Cruz, CA, USA).

391

392 **Mutant construction**

393 *Generation of mutants in E. coli:* Briefly, *E. coli* deletion or insertion mutants used in this
394 study originated either from the *E. coli* Keio collection of mutants (76) or were generated
395 by λ-red linear recombination using pKOBEG (Cm^R) or pKOBEGA (Amp^R) plasmids
396 (77) using primers listed in Sup. Table S5. P1vir transduction was used to transfer
397 mutations between different strains. When required, antibiotic resistance markers flanked
398 by two FRT sites were removed using the Flp recombinase (78). Plasmids used in this
399 study were constructed using an isothermal assembly method, Gibson assembly (New
400 England Biolabs, Ipswich, MA, USA) using primers listed in Sup. Table S5. The integrity
401 of all cloned fragments, mutations, and plasmids was verified by PCR with specific
402 primers and DNA sequencing

403

404 *Construction of deletion mutants*

405 Δ*yqiK*, Δ*qmcA*, Δ*hflK*, Δ*hflC*, Δ*clsA*, Δ*clsB*, Δ*clsC*,Δ*idi*, Δ*acrA*, Δ*cpoB* and Δ*dsbG*
406 deletions were transfered into *E. coli* MG1655*strep* by P1vir phage transduction from the
407 corresponding mutants in the *E. coli* BW25113 background of the Keio collection (76).
408 The associated kanamycin marker was then removed using the Flp recombinase
409 expressed from the plasmid pCP20 (78). (Details regarding the construction of all other
410 strains used in this study are presented in Sup. Table S4).

411

412 *Construction of GFP and mCherry* fusions

413 See Supplementary Materials and Methods section in Supplementary Materials
414
415 *Construction of complemented strains*
416 The *hflKC* or *yajC* genes were amplified from MG1655*strep* using primers listed in Sup.
417 Table S5 and cloned at the downstream of the IPTG-inducible promoter of a pZS*12
418 vector using the Gibson assembly to generate plasmids pZS*12-HflKC and pZS*12-YajC.
419 Then, these plasmids were introduced into Δ*hflKC* and Δ*yajC* mutants, respectively, to
420 construct complemented mutants (Sup. Table S4). A pZS*12 empty vector was also
421 introduced into wildtype, Δ*hflKC* and Δ*yajC* mutants. Mutants harbouring these pZS*12
422 plasmids were incubated and used for the below experiments in the presence of IPTG (1
423 mM) and ampicillin.
424
425 **Epifluorescence microscopy**
426 Bacteria were incubated into 5 mL of fresh LB medium and harvested at OD_{600} 0.4 for
427 samples in exponential phase or OD_{600} 2.0 for stationary phase. After washing twice with
428 M63B1 medium, cells corresponding to 1 mL of the bacterial culture were pelleted by
429 centrifugation and resuspended into 0.1 mL of M63B1 medium for exponential samples,
430 or 1 mL of the medium for stationary samples. Ten µL aliquots of the cell suspension
431 were immobilized on glass slides previously covered with freshly made M63B1 medium
432 0.8% agarose pads. Cells were observed using a ZEISS Definite focus fluorescent
433 microscope (Carl Zeiss, Oberkochen, Germany), equipped with an oil-immersion
434 objective lens microscope (Pln-Apo 63X/1.4 oil Ph3). GFP or mCherry fluorescence was
435 exited with a ZEISS Colibri LED illumination system and the fluorescence signal was
436 detected with Zeiss FS38 HE (Carl Zeiss) or Semrock HcRed filters (Semrock, Rochester,
437 NY, USA). GFP, and mCherry fluorescence images were taken at 1000, and 2000 msec.
438 exposure, respectively. Image processing was performed using ImageJ and Adobe
439 Photoshop. For each tested mutant, the subcellular localization patterns of 150 randomly
440 selected bacteria were evaluated and the frequencies were expressed as percentiles.
441
442 **Super resolution microscopy**
443 Bacteria were imaged using single-molecule localization microscopy and stochastic
444 optical reconstruction microscopy (SMLM-STORM), using a previously described

445 method (79). Overnight cultures were fixed with PFA 4%, permeabilized with Triton
446 0,05%, and labeled with either GFP monoclonal FluoTag®-Q — Sulfo-Cyanine 5 (Cy5),
447 or RFP monoclonal FluoTag®-Q – Cy5, which are single-domain antibodies (sdAb)
448 conjugated to Cy5. Labeling was performed at 1:250 (concentration), and washing steps
449 were carried out three times using Abbelight's SMART kit buffer. For imaging,
450 Abbelight's imaging system was used with NEO software. Abbelight's module was added
451 to an Olympus IX83 with 100x TIRF objective, N.A. 1.49. We used Hamamatsu's
452 sCMOS Flash 4 camera and a 647nm 500mW Oxxius laser, with an astigmatic lens, to
453 allow for 3D imaging of the sample (80).
454
455 **Inner membrane separation**
456 *E. coli* overnight cultures were diluted into 1 L of fresh LB medium to OD_{600} of 0.02, and
457 incubated at 37°C and 180 rpm until reaching OD_{600} 0.4. Cells were harvested and washed
458 once with 10 mM HEPES (pH 7.4) and stored at -20°C for at least 1 h. Bacteria were then
459 resuspended in 10 mL of 10 mM HEPES (pH 7.4) containing 100 µL of Benzonase (3.10^4
460 U/ml) and were passed through a FRENCH press (Thermo) at 20,000 psi. The lysate was
461 centrifugated at 15,000 *g* for 15 min at 4 °C to remove cell debris, and aliquots of the
462 suspension were stored at 4 °C as the whole extract. Then, the suspension was centrifuged
463 at 100,000 *g* for 45 min at 4 °C to separate supernatant and pellets, and aliquots of the
464 supernatant were stored at 4 °C as the cytosolic and periplasmic fractions. The pellets
465 were suspended into 600 µL of cold 10 mM HEPES (pH 7.4) and homogenized by using
466 2 mL tissue grinder (Kontes Glass, Vineland, NJ, USA). Discontinuous sucrose gradients
467 with the following composition were placed into ultracentrifugation tube: bottom to top
468 0.5 mL of 2 M sucrose, 2.0 mL of 1.5M sucrose, and 1.0 mL of 0.8 M sucrose, and 500
469 µL of the homogenized samples were placed on the top of sucrose gradients. The
470 gradients were centrifuged at 100,000 *g* for 17.5 h at 4 °C. Subsequently, 400 µL of
471 aliquots were collected into 11 microtubes from top to bottom, and the samples were
472 proceeded to the immunodetection method, as described below.
473
474 **Immunodetection of inner membrane proteins**
475 Aliquots of samples were suspended in 4× Laemmli buffer (BioRad) with 2-
476 Mercaptoethanol (Sigma) and incubated for 5 min at 98 °C. The protein samples (10 µL

477 each) were run on 4-20 % Mini-PROTEAN TGX Stain-FreeTM precast Gels (BioRad)
478 in 1× TGX buffer and then transferred to nitrocellulose membrane using a Trans-Blot®
479 Turbo™ Transfer System (BioRad). Subsequently, the membranes were blocked using
480 blocking buffer consisting of 5% skim milk in PBS with 0.05% Tween 20 (PBST) for 2
481 h at 4 °C with agitation. The membranes were then incubated in PBST containing 1%
482 skim milk with first antibodies, polyclonal rabbit antiserum raised against ExbB and TolC
483 (kindly given by Dr. Philippe Delepelaire), GFP (Invitrogen, A6455, Thermo Fisher
484 Scientific, Indianapolis, IN, USA) and mCherry (Invitrogen, PA5-34974) at 1:20,000
485 overnight at 4 °C with agitation. The membranes were washed in PBST and incubated in
486 PBST containing 1% skim milk with a secondary antibody, anti-rabbit IgG conjugated
487 with horseradish peroxidase (Cell signaling, 7074S), at 1:10,000 for 2 h at 25 °C with
488 agitation. After washing the excess secondary antibody, specific bands were visualized
489 using the ECL prime detection method (GE Healthcare) and imaged with an imaging
490 system, iBright^{TM} CL1500 (Invitrogen).
491
492 **Microbial growth phenotypic analysis**
493 A high-throughput analysis for microbial growth phenotypes using a colorimetric reaction,
494 Phenotype MicroArrays (Biolog Inc., Hayward, CA, USA), was performed in accordance
495 with the manufacturer's protocol. Briefly, several colonies of *E. coli* grown on LB agar
496 were transferred in 10 mL of a mixture of Biolog IF-0a media (BioLog) and sterilized
497 water into a sterile capped test tube. The suspension was mixed gently, and the turbidity
498 was adjusted to achieve the appropriate transmittance using the Biolog turbidimeter
499 (BioLog). The cell suspension was diluted with the IF-0a plus dye mix, as mentioned in
500 the manufacturer's protocol. 100 µL of the mixture suspension was inoculated into PM
501 plates 1-3 and 9-20 and incubated for 72 h at 37 °C. The absorbance of each well was
502 taken every 15 min. The OmniLog software (BioLog) was used to view and edit data, to
503 compare data lists, and to generate reports.
504
505 **Monitoring of bacterial growth**
506 An overnight culture of *E. coli* was diluted into fresh LB and M63B1 supplemented with
507 0.4% glucose medium to OD_{600} of 0.05, and 200 µL aliquots were cultured in the presence
508 or absence of paraquat (Methyl viologen dichloride hydrate, Sigma-Aldrich) in 96-well

509 microplates at 37 °C for 24 h with shaking. The absorbance of each culture at 600 nm was
510 measured every 15 min for 24 h using a microplate reader (Tecan Infinite, Mannedorf,
511 Switzerland).
512
513 **Susceptibility of *E. coli* against Tobramycin and Paraquat**
514 The broth microdilution method was used to determine the MIC (minimum inhibitory
515 concentration) values of Tobramycin (Sigma-Aldrich) and Paraquat (Sigma-Aldrich) in
516 96-well microtiter plates. Briefly, 100 µL of LB medium was distributed into each well
517 of the microtiter plates. Tobramycin was 2-fold serially diluted in each well. Five µL of
518 approximately 1×10^7 CFU/mL of *E. coli* was inoculated into each well, and the plates
519 were incubated at 37°C for 24 h. The lowest concentration that visibly inhibited bacterial
520 growth was defined as the MIC. All strains were evaluated in biological and technical
521 triplicates.
522 The spot assay was performed to evaluate the susceptibility of *E. coli* against
523 paraquat. Briefly, an overnight culture of *E. coli* was diluted into fresh LB medium to
524 OD_{600} of 0.05. Ten µL of the diluted culture was spotted on LB plates containing either
525 no or 100 µM paraquat. The plates were incubated at 37°C for 24 h, and the photographs
526 were taken. All strains were evaluated in triplicate.
527
528 **HflC-tag protein-protein interaction assay**
529
530 *Construction and growth behavior of the E. coli HflC-tag strain and growth phase*
531 *dependent expression of HflC*
532 The *hflC* gene was chromosomally tagged at its 3'end with the coding sequence for a
533 double affinity TAG, creating a translation fusion with a Twin-Strep-Tag and a 6 x His-
534 poly-histidine-Tag at the C-terminus of HflC. A 3' located kanamycin resistance cassette
535 was co-integrated with the double-Tag sequence and positive clones were selected on
536 kanamycin selective LB agar plates (50 µg/mL Km) and verified by DNA sequencing.
537 The cloning strategy and primers used for the chromosomal integration construct can be
538 found in in the Mutant construction section and Table S5. The double-affinity-Tag
539 strategy enables a two-step purification to minimize co-purification of unspecifically
540 bound proteins from the first purification step if necessary. To analyze the expression

541 pattern of the tagged HflC variant, the strain was cultivated in unlabeled 14N
542 BioExpress®1000 complex medium (CGM-1000-U - Cambridge Isotope Laboratories,
543 Inc.). Exponentially growing cells from an overnight pre-culture were used to inoculate
544 the main culture to a starting OD_{600} of 0.05 and growth was monitored up to 2 hours after
545 entry into stationary phase (Sup. Fig S10). Growth phase dependent expression of HflC-
546 tag was monitored by fluorescent Western blot detection using a CW800-Cy-dye labeled
547 StrepTactinXT conjugate on a LI-COR Odyssey CLx scanner (Sup. Fig S10).
548 Quantification of Western blot signals with the Image Studio software (LI-COR) showed
549 that HflC was uniformly and strongly expressed across all growth phases. To identify
550 potential interaction partners of HflC early exponential growth phase (OD_{600} 0.4) and
551 stationary phase (~ OD_{600} 5.5 or 1 h after entry into stat. phase) samples were selected for
552 further testing.
553
554 *$^{14}N/^{15}N$ stable isotope labeling, formaldehyde cross-linking and cell sampling*
555 The *E. coli* wild-type strain was cultivated in both, unlabeled ^{14}N-BioExpress®1000
556 medium (CGM-1000-U) as well as stable isotope labeled ^{15}N-BioExpress®medium
557 (CGM-1000-N) from Cambridge Isotope Laboratories, Inc. The *E. coli* HflC-tag strain
558 was only cultivated in unlabeled ^{14}N-BioExpress®1000 medium. All experiments were
559 performed in quadruplicate biological replicates. Each main culture was inoculated from
560 exponentially growing precultures grown in the corresponding ^{14}N or ^{15}N labeled medium
561 to a starting OD_{600} of 0.05. When the cultures reached an optical density of 0.4 or 60 min
562 of stationary phase (~ OD_{600} 5.5) 16 OD units were either immediately harvested by
563 centrifugation (non-crosslinked samples) or mixed with a freshly prepared
564 Paraformaldehyde solution (4%) to a final concentration of 0.6% and incubated for 25
565 min at 37°C (crosslinked samples) (81, 82). The chemical cross-linking of proteins using
566 formaldehyde has a very short cross-linking span (~2-3 Å) making it an ideal tool for
567 detecting specific protein-protein interactions with great confidence (83). After cross-
568 linking cells were harvested by centrifugation at room temperature for 2 min at 5000 rpm.
569 The pellets were frozen in liquid nitrogen and stored at -80°C for further preparation.
570
571 *Cell disruption and affinity Tag purification*

572 The pellets were resuspended in 250 µL 20 mM HEPES pH 8.0 and mechanically
573 disrupted in the frozen state using a bead mill. The powder of disrupted cells was then
574 mixed with another 250 µL of HEPES buffer and a nuclease digestion was performed.
575 The lysates were not centrifuged, and a protein assay (BCA) was performed from the
576 crude lysates at a 1:50 dilution in 20mM HEPES pH8.0 with 1% SDS. For affinity
577 purification using Strep-Tactin® Magnetic Microbeads (IBA Lifesciences GmbH,
578 Goettingen, Germany), 750 µg of crude lysate of each sample were used and mixed with
579 2x concentrated wash buffer (20 mM HEPES pH 8.0 + 30% Sarcosyl) at a 1:1 volume
580 ratio and filled up to 800 µL with 1x wash buffer (20 mM HEPES pH8.0 + 15% Sarcosyl).
581 In parallel, 150 µL of each bead suspension was equilibrated 3 x with 1x wash buffer
582 (equivalent to 7.5 µL beads) and the pellet was then mixed with the respective lysate
583 (vortexed briefly) and then incubated on an overhead shaker (IKA™ Loopster Digital,
584 Fisher scientic) at level 9 at room temperature for 1 h. Purification was then performed in
585 the magnet rack. Samples were washed 4 times with 600 µL wash buffer and separated
586 from the supernatants using the magnet rack. Elution was performed in 50 µL 20 mM
587 HEPES pH 8.0 with 100 mM biotin without Sarcosyl.
588
589 *SDS-PAGE, Western blot evaluation, quantification and ratio determination of $^{14}N/^{15}N$*
590 *isotope labeled purified samples*
591 For the Western blot experiments, 4 µL of the purified eluates from exponential and
592 stationary growth was separated by SDS-PAGE (Nu-PAGE gradient gels 4 - 12%) and
593 transferred to a low fluorescent PVDF membrane with a BioRad Turbo Blot System (Sup.
594 Fig S11A and B). In order to distinguish non-specifically purified and cross-linked
595 proteins from true interaction partners, ^{14}N and ^{15}N labeled samples were mixed with
596 respect to AccB signal intensity from the Western blots in a ratio of 1:1. Thus, the heavily
597 labeled ^{15}N pool or reference sample was used in a constant amount of 130 ng per mass
598 spectrometric measurement and was mixed with the corresponding volume of each ^{14}N
599 sample of the *E. coli* wild type as well as the *E. coli* HflC-tag samples (Sup. Fig S11A
600 and B).
601

602 **Mass spectrometry and data evaluation of $^{14}N/^{15}N$ isotope labeled samples**

603 Samples were digested and analyzed by mass spectrometry. Data were analyzed using
604 Spectronaut 15 (directDIA, FDR = 0.01) and filtered for an ion Q-value below 0.001.
605 Protein ratios were calculated using the median of light/heavy peptide ratios per protein.
606 Protein ratios were then normalized using AccB ratios as reference. The statistical
607 analysis was performed using an empirical Bayes t-test (limma package 3.50.3) (84) and
608 multiple test adjustment utilizing the Benjamini-Hochberg approach. The criteria for
609 significance of a potential interaction are based on an identification of the protein in at
610 least 3 of the 4 replicates with more than 2 identified peptides per protein, a q-value below
611 0.05, and a calculated ratio (fold change or enrichment factor) of at least 32-fold. Proteins
612 that were also enriched from the wildtype control, that did not contain affinity tagged
613 proteins, represent unspecific resin interactions and were removed from the list of HflC
614 interaction partners (Sup. Fig. S8 and Sup Table S2 and 3). Supplementary Table S6 and
615 S7 summarize the reversed phase liquid chromatography (RPLC) as well as the mass
616 spectrometry method used.
617
618 **Statistical analysis**

619 Data analysis was performed using GraphPad Prism 6.0 software (GraphPad, La Jolla,
620 CA, USA). All data are expressed as mean (± standard deviation, SD) in figures.
621 Statistical analysis was performed using Two-tailed unpaired *t-test* with Welch correction.
622 Differences were considered statistically significant for P values of <0.05.

ACKNOWLEDGMENTS

We thank Philippe Delepelaire for insightful comments and material support. We are grateful to Eva Wolrab and Sven van Teeffelen for their initial interest in the project and for providing the strains for msfGFP and mCherry constructions. We thank Uwe Sauer and Philip Warmer for initial assessment of lipid composition of some of the strains used in this study. This work was supported by EU Horizon 2020 Rafts4Biotech grant 720776 (to JMG, DL, AKW, YY, AR, UV and MS), the French government's Investissement d'Avenir Program, Laboratoire d'Excellence "Integrative Biology of Emerging Infectious Diseases" (grant n°ANR-10-LABX-62-IBEID) and the *Fondation pour la Recherche Médicale* (grant no. DEQ20180339185). This work benefited from the facilities and expertise of Add Photonic BioImaging platform (UTechS PBI, Institut Pasteur). A.K.W. was supported by a Pasteur-Roux-Cantarini postdoctoral and a grant from the Philippe Foundation.

AUTHOR CONTRIBUTIONS:

A.K.W., Y.Y., and J.-M.G. designed the experiments. A.K.W., Y.Y., A.R., R.B.; M.S., J.B-B. performed the experiments. A.K.W., Y.Y., A.R., U.V. M.S., R.B., J.-M.B., C.B., D.L. and J.-M.G. analyzed the data. Y.Y., A.K.W. and J.-M.G. wrote the paper with significant contribution from all authors.

647 **REFERENCES**
648

649 1. **Alberts B, Johnson A, Lewis J, Raff M, Roberts K, Walter P.** 2002.
650 Molecular biology of the cell 6th edition ed. Garland Science., New York.
651 2. **Cho W, Stahelin RV.** 2005. Membrane-protein interactions in cell signaling
652 and membrane trafficking. Annu Rev Biophys Biomol Struct **34:**119-
653 151.10.1146/annurev.biophys.33.110502.133337:
654 10.1146/annurev.biophys.33.110502.133337
655 3. **Simons K, Ikonen E.** 1997. Functional rafts in cell membranes. Nature
656 **387:**569-572.10.1038/42408: 10.1038/42408
657 4. **Rajendran L, Simons K.** 2005. Lipid rafts and membrane dynamics. J Cell Sci
658 **118:**1099-1102.10.1242/jcs.01681: 10.1242/jcs.01681
659 5. **Simons K, Sampaio JL.** 2011. Membrane organization and lipid rafts. Cold
660 Spring Harb Perspect Biol **3:**a004697.10.1101/cshperspect.a004697:
661 10.1101/cshperspect.a004697
662 6. **Pike LJ.** 2006. Rafts defined: a report on the Keystone Symposium on Lipid
663 Rafts and Cell Function. J Lipid Res **47:**1597-1598.10.1194/jlr.E600002-
664 JLR200: 10.1194/jlr.E600002-JLR200
665 7. **Sezgin E, Levental I, Mayor S, Eggeling C.** 2017. The mystery of membrane
666 organization: composition, regulation and roles of lipid rafts. Nat Rev Mol Cell
667 Biol **18:**361-374.10.1038/nrm.2017.16: 10.1038/nrm.2017.16
668 8. **Langhorst MF, Reuter A, Stuermer CA.** 2005. Scaffolding microdomains and
669 beyond: the function of reggie/flotillin proteins. Cell Mol Life Sci **62:**2228-
670 2240.10.1007/s00018-005-5166-4: 10.1007/s00018-005-5166-4
671 9. **Morrow IC, Parton RG.** 2005. Flotillins and the PHB domain protein family:
672 rafts, worms and anaesthetics. Traffic **6:**725-740.10.1111/j.1600-
673 0854.2005.00318.x: 10.1111/j.1600-0854.2005.00318.x
674 10. **Stuermer CA, Plattner H.** 2005. The 'lipid raft' microdomain proteins reggie-1
675 and reggie-2 (flotillins) are scaffolds for protein interaction and signalling.
676 Biochem Soc Symp**:**109-118.10.1042/bss0720109: 10.1042/bss0720109
677 11. **Browman DT, Hoegg MB, Robbins SM.** 2007. The SPFH domain-containing
678 proteins: more than lipid raft markers. Trends Cell Biol **17:**394-
679 402.10.1016/j.tcb.2007.06.005: 10.1016/j.tcb.2007.06.005
680 12. **Zeke A, Lukács M, Lim WA, Reményi A.** 2009. Scaffolds: interaction
681 platforms for cellular signalling circuits. Trends Cell Biol **19:**364-
682 374.10.1016/j.tcb.2009.05.007: 10.1016/j.tcb.2009.05.007
683 13. **Zhao F, Zhang J, Liu YS, Li L, He YL.** 2011. Research advances on flotillins.
684 Virol J **8:**479.10.1186/1743-422x-8-479: 10.1186/1743-422x-8-479
685 14. **Lopez D, Koch G.** 2017. Exploring functional membrane microdomains in
686 bacteria: an overview. Curr Opin Microbiol **36:**76-
687 84.10.1016/j.mib.2017.02.001: 10.1016/j.mib.2017.02.001
688 15. **Lopez D, Kolter R.** 2010. Functional microdomains in bacterial membranes.
689 Genes Dev **24:**1893-1902.10.1101/gad.1945010: 10.1101/gad.1945010
690 16. **Bramkamp M, Lopez D.** 2015. Exploring the existence of lipid rafts in
691 bacteria. Microbiol Mol Biol Rev **79:**81-100.10.1128/mmbr.00036-14:
692 10.1128/mmbr.00036-14

17. **Willdigg JR, Helmann JD.** 2021. Mini Review: Bacterial Membrane Composition and Its Modulation in Response to Stress. Front Mol Biosci **8:**634438.10.3389/fmolb.2021.634438: 10.3389/fmolb.2021.634438
18. **Dempwolff F, Möller HM, Graumann PL.** 2012. Synthetic motility and cell shape defects associated with deletions of flotillin/reggie paralogs in Bacillus subtilis and interplay of these proteins with NfeD proteins. J Bacteriol **194:**4652-4661.10.1128/jb.00910-12: 10.1128/jb.00910-12
19. **Bach JN, Bramkamp M.** 2013. Flotillins functionally organize the bacterial membrane. Mol Microbiol **88:**1205-1217.10.1111/mmi.12252: 10.1111/mmi.12252
20. **Schneider J, Klein T, Mielich-Süss B, Koch G, Franke C, Kuipers OP, Kovács Á T, Sauer M, Lopez D.** 2015. Spatio-temporal remodeling of functional membrane microdomains organizes the signaling networks of a bacterium. PLoS Genet **11:**e1005140.10.1371/journal.pgen.1005140: 10.1371/journal.pgen.1005140
21. **Wagner RM, Kricks L, Lopez D.** 2017. Functional Membrane Microdomains Organize Signaling Networks in Bacteria. J Membr Biol **250:**367-378.10.1007/s00232-016-9923-0: 10.1007/s00232-016-9923-0
22. **Donovan C, Bramkamp M.** 2009. Characterization and subcellular localization of a bacterial flotillin homologue. Microbiology **155:**1786-1799.10.1099/mic.0.025312-0: 10.1099/mic.0.025312-0
23. **Yepes A, Schneider J, Mielich B, Koch G, García-Betancur JC, Ramamurthi KS, Vlamakis H, López D.** 2012. The biofilm formation defect of a Bacillus subtilis flotillin-defective mutant involves the protease FtsH. Mol Microbiol **86:**457-471.10.1111/j.1365-2958.2012.08205.x: 10.1111/j.1365-2958.2012.08205.x
24. **Mielich-Süss B, Schneider J, Lopez D.** 2013. Overproduction of flotillin influences cell differentiation and shape in Bacillus subtilis. mBio **4:**e00719-00713.10.1128/mBio.00719-13: 10.1128/mBio.00719-13
25. **Schneider J, Mielich-Süss B, Böhme R, Lopez D.** 2015. In vivo characterization of the scaffold activity of flotillin on the membrane kinase KinC of Bacillus subtilis. Microbiology **161:**1871-1887.10.1099/mic.0.000137: 10.1099/mic.0.000137
26. **Hinderhofer M, Walker CA, Friemel A, Stuermer CA, Möller HM, Reuter A.** 2009. Evolution of prokaryotic SPFH proteins. BMC Evol Biol **9:**10.10.1186/1471-2148-9-10: 10.1186/1471-2148-9-10
27. **Kihara A, Akiyama Y, Ito K.** 1996. A protease complex in the Escherichia coli plasma membrane: HflKC (HflA) forms a complex with FtsH (HflB), regulating its proteolytic activity against SecY. Embo j **15:**6122-6131
28. **Saikawa N, Akiyama Y, Ito K.** 2004. FtsH exists as an exceptionally large complex containing HflKC in the plasma membrane of Escherichia coli. J Struct Biol **146:**123-129.10.1016/j.jsb.2003.09.020: 10.1016/j.jsb.2003.09.020
29. **Chiba S, Ito K, Akiyama Y.** 2006. The Escherichia coli plasma membrane contains two PHB (prohibitin homology) domain protein complexes of opposite orientations. Mol Microbiol **60:**448-457.10.1111/j.1365-2958.2006.05104.x: 10.1111/j.1365-2958.2006.05104.x
30. **Ma C, Wang C, Luo D, Yan L, Yang W, Li N, Gao N.** 2022. Structural insights into the membrane microdomain organization by SPFH family proteins.

741 Cell Res **32:**176-189.10.1038/s41422-021-00598-3: 10.1038/s41422-021-
742 00598-3
743 31. **Brown DA, Rose JK.** 1992. Sorting of GPI-anchored proteins to glycolipid-
744 enriched membrane subdomains during transport to the apical cell surface. Cell
745 **68:**533-544.10.1016/0092-8674(92)90189-j: 10.1016/0092-8674(92)90189-j
746 32. **Schroeder R, London E, Brown D.** 1994. Interactions between saturated acyl
747 chains confer detergent resistance on lipids and glycosylphosphatidylinositol
748 (GPI)-anchored proteins: GPI-anchored proteins in liposomes and cells show
749 similar behavior. Proc Natl Acad Sci U S A **91:**12130-
750 12134.10.1073/pnas.91.25.12130: 10.1073/pnas.91.25.12130
751 33. **Lichtenberg D, Goñi FM, Heerklotz H.** 2005. Detergent-resistant membranes
752 should not be identified with membrane rafts. Trends Biochem Sci **30:**430-
753 436.10.1016/j.tibs.2005.06.004: 10.1016/j.tibs.2005.06.004
754 34. **Brown DA.** 2006. Lipid rafts, detergent-resistant membranes, and raft targeting
755 signals. Physiology (Bethesda) **21:**430-439.10.1152/physiol.00032.2006:
756 10.1152/physiol.00032.2006
757 35. **Guzmán-Flores JE, Steinemann-Hernández L, González de la Vara LE,**
758 **Gavilanes-Ruiz M, Romeo T, Alvarez AF, Georgellis D.** 2019. Proteomic
759 analysis of Escherichia coli detergent-resistant membranes (DRM). PLoS One
760 **14:**e0223794.10.1371/journal.pone.0223794: 10.1371/journal.pone.0223794
761 36. **Guzman-Flores JE, Alvarez AF, Poggio S, Gavilanes-Ruiz M, Georgellis D.**
762 2017. Isolation of detergent-resistant membranes (DRMs) from Escherichia coli.
763 Anal Biochem **518:**1-8.10.1016/j.ab.2016.10.025: 10.1016/j.ab.2016.10.025
764 37. **Ito K, Akiyama Y.** 2005. Cellular functions, mechanism of action, and
765 regulation of FtsH protease. Annu Rev Microbiol **59:**211-
766 231.10.1146/annurev.micro.59.030804.121316:
767 10.1146/annurev.micro.59.030804.121316
768 38. **Padilla-Vaca F, Vargas-Maya NI, Elizarrarás-Vargas NU, Rangel-Serrano**
769 **Á, Cardoso-Reyes LR, Razo-Soria T, Membrillo-Hernández J, Franco B.**
770 2019. Flotillin homologue is involved in the swimming behavior of Escherichia
771 coli. Arch Microbiol **201:**999-1008.10.1007/s00203-019-01670-8:
772 10.1007/s00203-019-01670-8
773 39. **Romantsov T, Helbig S, Culham DE, Gill C, Stalker L, Wood JM.** 2007.
774 Cardiolipin promotes polar localization of osmosensory transporter ProP in
775 Escherichia coli. Mol Microbiol **64:**1455-1465.10.1111/j.1365-
776 2958.2007.05727.x: 10.1111/j.1365-2958.2007.05727.x
777 40. **Mileykovskaya E, Dowhan W.** 2009. Cardiolipin membrane domains in
778 prokaryotes and eukaryotes. Biochim Biophys Acta **1788:**2084-
779 2091.10.1016/j.bbamem.2009.04.003: 10.1016/j.bbamem.2009.04.003
780 41. **Feng X, Hu Y, Zheng Y, Zhu W, Li K, Huang CH, Ko TP, Ren F, Chan**
781 **HC, Nega M, Bogue S, López D, Kolter R, Götz F, Guo RT, Oldfield E.**
782 2014. Structural and functional analysis of Bacillus subtilis YisP reveals a role
783 of its product in biofilm production. Chem Biol **21:**1557-
784 1563.10.1016/j.chembiol.2014.08.018: 10.1016/j.chembiol.2014.08.018
785 42. **Zielińska A, Savietto A, de Sousa Borges A, Martinez D, Berbon M,**
786 **Roelofsen JR, Hartman AM, de Boer R, van der Klei IJ, Hirsch AKH,**
787 **Habenstein B, Bramkamp M, Scheffers D-J.** 2020. Flotillin mediated

788 membrane fluidity controls peptidoglycan synthesis and MreB movement.
789 bioRxiv:736819.10.1101/736819: 10.1101/736819
790 43. **Nishijima S, Asami Y, Uetake N, Yamagoe S, Ohta A, Shibuya I.** 1988.
791 Disruption of the Escherichia coli cls gene responsible for cardiolipin synthesis.
792 J Bacteriol **170:**775-780.10.1128/jb.170.2.775-780.1988: 10.1128/jb.170.2.775-
793 780.1988
794 44. **Hahn FM, Hurlburt AP, Poulter CD.** 1999. Escherichia coli open reading
795 frame 696 is idi, a nonessential gene encoding isopentenyl diphosphate
796 isomerase. J Bacteriol **181:**4499-4504
797 45. **Aires JR, Nikaido H.** 2005. Aminoglycosides are captured from both periplasm
798 and cytoplasm by the AcrD multidrug efflux transporter of Escherichia coli. J
799 Bacteriol **187:**1923-1929.10.1128/jb.187.6.1923-1929.2005:
800 10.1128/jb.187.6.1923-1929.2005
801 46. **Samuelson JC, Chen M, Jiang F, Möller I, Wiedmann M, Kuhn A, Phillips**
802 **GJ, Dalbey RE.** 2000. YidC mediates membrane protein insertion in bacteria.
803 Nature **406:**637-641.10.1038/35020586: 10.1038/35020586
804 47. **Urbanus ML, Fröderberg L, Drew D, Björk P, de Gier JW, Brunner J,**
805 **Oudega B, Luirink J.** 2002. Targeting, insertion, and localization of
806 Escherichia coli YidC. J Biol Chem **277:**12718-
807 12723.10.1074/jbc.M200311200: 10.1074/jbc.M200311200
808 48. **Tavernarakis N, Driscoll M, Kyrpides NC.** 1999. The SPFH domain:
809 implicated in regulating targeted protein turnover in stomatins and other
810 membrane-associated proteins. Trends Biochem Sci **24:**425-427.10.1016/s0968-
811 0004(99)01467-x: 10.1016/s0968-0004(99)01467-x
812 49. **Morrow IC, Rea S, Martin S, Prior IA, Prohaska R, Hancock JF, James**
813 **DE, Parton RG.** 2002. Flotillin-1/reggie-2 traffics to surface raft domains via a
814 novel golgi-independent pathway. Identification of a novel membrane targeting
815 domain and a role for palmitoylation. J Biol Chem **277:**48834-
816 48841.10.1074/jbc.M209082200: 10.1074/jbc.M209082200
817 50. **Dempwolff F, Schmidt FK, Hervás AB, Stroh A, Rösch TC, Riese CN,**
818 **Dersch S, Heimerl T, Lucena D, Hülsbusch N, Stuermer CA, Takeshita N,**
819 **Fischer R, Eckhardt B, Graumann PL.** 2016. Super Resolution Fluorescence
820 Microscopy and Tracking of Bacterial Flotillin (Reggie) Paralogs Provide
821 Evidence for Defined-Sized Protein Microdomains within the Bacterial
822 Membrane but Absence of Clusters Containing Detergent-Resistant Proteins.
823 PLoS Genet **12:**e1006116.10.1371/journal.pgen.1006116:
824 10.1371/journal.pgen.1006116
825 51. **Somani VK, Aggarwal S, Singh D, Prasad T, Bhatnagar R.** 2016.
826 Identification of Novel Raft Marker Protein, FlotP in Bacillus anthracis. Front
827 Microbiol **7:**169.10.3389/fmicb.2016.00169: 10.3389/fmicb.2016.00169
828 52. **García-Fernández E, Koch G, Wagner RM, Fekete A, Stengel ST,**
829 **Schneider J, Mielich-Süss B, Geibel S, Markert SM, Stigloher C, Lopez D.**
830 2017. Membrane Microdomain Disassembly Inhibits MRSA Antibiotic
831 Resistance. Cell **171:**1354-1367.e1320.10.1016/j.cell.2017.10.012:
832 10.1016/j.cell.2017.10.012
833 53. **Dempwolff F, Wischhusen HM, Specht M, Graumann PL.** 2012. The
834 deletion of bacterial dynamin and flotillin genes results in pleiotrophic effects on

835 cell division, cell growth and in cell shape maintenance. BMC Microbiol
836 **12:**298.10.1186/1471-2180-12-298: 10.1186/1471-2180-12-298
837 54. **Yokoyama H, Matsui I.** 2020. The lipid raft markers stomatin, prohibitin,
838 flotillin, and HflK/C (SPFH)-domain proteins form an operon with NfeD
839 proteins and function with apolar polyisoprenoid lipids. Crit Rev Microbiol
840 **46:**38-48.10.1080/1040841x.2020.1716682: 10.1080/1040841x.2020.1716682
841 55. **Kihara A, Ito K.** 1998. Translocation, folding, and stability of the HflKC
842 complex with signal anchor topogenic sequences. J Biol Chem **273:**29770-
843 29775.10.1074/jbc.273.45.29770: 10.1074/jbc.273.45.29770
844 56. **Edgar R, Rokney A, Feeney M, Semsey S, Kessel M, Goldberg MB, Adhya**
845 **S, Oppenheim AB.** 2008. Bacteriophage infection is targeted to cellular poles.
846 Mol Microbiol **68:**1107-1116.10.1111/j.1365-2958.2008.06205.x:
847 10.1111/j.1365-2958.2008.06205.x
848 57. **Bandyopadhyay K, Parua PK, Datta AB, Parrack P.** 2010. Escherichia coli
849 HflK and HflC can individually inhibit the HflB (FtsH)-mediated proteolysis of
850 lambdaCII in vitro. Arch Biochem Biophys **501:**239-
851 243.10.1016/j.abb.2010.06.030: 10.1016/j.abb.2010.06.030
852 58. **Raetz CR, Dowhan W.** 1990. Biosynthesis and function of phospholipids in
853 Escherichia coli. J Biol Chem **265:**1235-1238
854 59. **Lin TY, Weibel DB.** 2016. Organization and function of anionic phospholipids
855 in bacteria. Appl Microbiol Biotechnol **100:**4255-4267.10.1007/s00253-016-
856 7468-x: 10.1007/s00253-016-7468-x
857 60. **Sohlenkamp C, Geiger O.** 2016. Bacterial membrane lipids: diversity in
858 structures and pathways. FEMS Microbiol Rev **40:**133-
859 159.10.1093/femsre/fuv008: 10.1093/femsre/fuv008
860 61. **El Khoury M, Swain J, Sautrey G, Zimmermann L, Van Der Smissen P,**
861 **Décout JL, Mingeot-Leclercq MP.** 2017. Targeting Bacterial Cardiolipin
862 Enriched Microdomains: An Antimicrobial Strategy Used by Amphiphilic
863 Aminoglycoside Antibiotics. Sci Rep **7:**10697.10.1038/s41598-017-10543-3:
864 10.1038/s41598-017-10543-3
865 62. **Oliver PM, Crooks JA, Leidl M, Yoon EJ, Saghatelian A, Weibel DB.** 2014.
866 Localization of anionic phospholipids in Escherichia coli cells. J Bacteriol
867 **196:**3386-3398.10.1128/jb.01877-14: 10.1128/jb.01877-14
868 63. **Romantsov T, Stalker L, Culham DE, Wood JM.** 2008. Cardiolipin controls
869 the osmotic stress response and the subcellular location of transporter ProP in
870 Escherichia coli. J Biol Chem **283:**12314-12323.10.1074/jbc.M709871200:
871 10.1074/jbc.M709871200
872 64. **Arias-Cartin R, Grimaldi S, Arnoux P, Guigliarelli B, Magalon A.** 2012.
873 Cardiolipin binding in bacterial respiratory complexes: structural and functional
874 implications. Biochim Biophys Acta **1817:**1937-
875 1949.10.1016/j.bbabio.2012.04.005: 10.1016/j.bbabio.2012.04.005
876 65. **Romantsov T, Gonzalez K, Sahtout N, Culham DE, Coumoundouros C,**
877 **Garner J, Kerr CH, Chang L, Turner RJ, Wood JM.** 2018. Cardiolipin
878 synthase A colocalizes with cardiolipin and osmosensing transporter ProP at the
879 poles of Escherichia coli cells. Mol Microbiol **107:**623-638.10.1111/mmi.13904:
880 10.1111/mmi.13904
881 66. **van Tilburg AY, Warmer P, van Heel AJ, Sauer U, Kuipers OP.** 2022.
882 Membrane composition and organization of Bacillus subtilis 168 and its

883 genome-reduced derivative miniBacillus PG10. Microb Biotechnol **15:**1633-
884 1651.10.1111/1751-7915.13978: 10.1111/1751-7915.13978
885 67. **Akiyama Y.** 2009. Quality control of cytoplasmic membrane proteins in
886 Escherichia coli. J Biochem **146:**449-454.10.1093/jb/mvp071:
887 10.1093/jb/mvp071
888 68. **Hinz A, Lee S, Jacoby K, Manoil C.** 2011. Membrane proteases and
889 aminoglycoside antibiotic resistance. J Bacteriol **193:**4790-
890 4797.10.1128/jb.05133-11: 10.1128/jb.05133-11
891 69. **Venter H, Mowla R, Ohene-Agyei T, Ma S.** 2015. RND-type drug efflux
892 pumps from Gram-negative bacteria: molecular mechanism and inhibition. Front
893 Microbiol **6:**377.10.3389/fmicb.2015.00377: 10.3389/fmicb.2015.00377
894 70. **Nikaido E, Shirosaka I, Yamaguchi A, Nishino K.** 2011. Regulation of the
895 AcrAB multidrug efflux pump in Salmonella enterica serovar Typhimurium in
896 response to indole and paraquat. Microbiology **157:**648-
897 655.10.1099/mic.0.045757-0: 10.1099/mic.0.045757-0
898 71. **Garneau-Tsodikova S, Labby KJ.** 2016. Mechanisms of Resistance to
899 Aminoglycoside Antibiotics: Overview and Perspectives. Medchemcomm **7:**11-
900 27.10.1039/c5md00344j: 10.1039/c5md00344j
901 72. **Pogliano KJ, Beckwith J.** 1994. Genetic and molecular characterization of the
902 Escherichia coli secD operon and its products. J Bacteriol **176:**804-
903 814.10.1128/jb.176.3.804-814.1994: 10.1128/jb.176.3.804-814.1994
904 73. **Kato Y, Nishiyama K, Tokuda H.** 2003. Depletion of SecDF-YajC causes a
905 decrease in the level of SecG: implication for their functional interaction. FEBS
906 Lett **550:**114-118.10.1016/s0014-5793(03)00847-0: 10.1016/s0014-
907 5793(03)00847-0
908 74. **Crane JM, Randall LL.** 2017. The Sec System: Protein Export in Escherichia
909 coli. EcoSal Plus **7**.10.1128/ecosalplus.ESP-0002-2017:
910 10.1128/ecosalplus.ESP-0002-2017
911 75. **Törnroth-Horsefield S, Gourdon P, Horsefield R, Brive L, Yamamoto N,**
912 **Mori H, Snijder A, Neutze R.** 2007. Crystal structure of AcrB in complex with
913 a single transmembrane subunit reveals another twist. Structure **15:**1663-
914 1673.10.1016/j.str.2007.09.023: 10.1016/j.str.2007.09.023
915 76. **Baba T, Ara T, Hasegawa M, Takai Y, Okumura Y, Baba M, Datsenko KA,**
916 **Tomita M, Wanner BL, Mori H.** 2006. Construction of Escherichia coli K-12
917 in-frame, single-gene knockout mutants: the Keio collection. Mol Syst Biol
918 **2:**2006.0008.10.1038/msb4100050: 10.1038/msb4100050
919 77. **Chaveroche MK, Ghigo JM, d'Enfert C.** 2000. A rapid method for efficient
920 gene replacement in the filamentous fungus Aspergillus nidulans. Nucleic Acids
921 Res **28:**E97.10.1093/nar/28.22.e97: 10.1093/nar/28.22.e97
922 78. **Cherepanov PP, Wackernagel W.** 1995. Gene disruption in Escherichia coli:
923 TcR and KmR cassettes with the option of Flp-catalyzed excision of the
924 antibiotic-resistance determinant. Gene **158:**9-14.10.1016/0378-1119(95)00193-
925 a: 10.1016/0378-1119(95)00193-a
926 79. **Boudjemaa R, Cabriel C, Dubois-Brissonnet F, Bourg N, Dupuis G, Gruss**
927 **A, Leveque-Fort S, Briandet R, Fontaine-Aupart MP, Steenkeste K.** 2018.
928 Impact of Bacterial Membrane Fatty Acid Composition on the Failure of
929 Daptomycin To Kill Staphylococcus aureus. Antimicrob Agents Chemother
930 **62**.10.1128/AAC.00023-18: 10.1128/AAC.00023-18

80. **Cabriel C, Bourg N, Dupuis G, Leveque-Fort S.** 2018. Aberration-accounting calibration for 3D single-molecule localization microscopy. Opt Lett **43:**174-177.10.1364/OL.43.000174: 10.1364/OL.43.000174

81. **Herzberg C, Weidinger LA, Dörrbecker B, Hübner S, Stülke J, Commichau FM.** 2007. SPINE: a method for the rapid detection and analysis of protein-protein interactions in vivo. Proteomics **7:**4032-4035.10.1002/pmic.200700491: 10.1002/pmic.200700491

82. **Müller VS, Jungblut PR, Meyer TF, Hunke S.** 2011. Membrane-SPINE: an improved method to identify protein-protein interaction partners of membrane proteins in vivo. Proteomics **11:**2124-2128.10.1002/pmic.201000558: 10.1002/pmic.201000558

83. **Sutherland BW, Toews J, Kast J.** 2008. Utility of formaldehyde cross-linking and mass spectrometry in the study of protein-protein interactions. J Mass Spectrom **43:**699-715.10.1002/jms.1415: 10.1002/jms.1415

84. **Ritchie ME, Phipson B, Wu D, Hu Y, Law CW, Shi W, Smyth GK.** 2015. limma powers differential expression analyses for RNA-sequencing and microarray studies. Nucleic Acids Res **43:**e47.10.1093/nar/gkv007: 10.1093/nar/gkv007

950 **FIGURES**

951

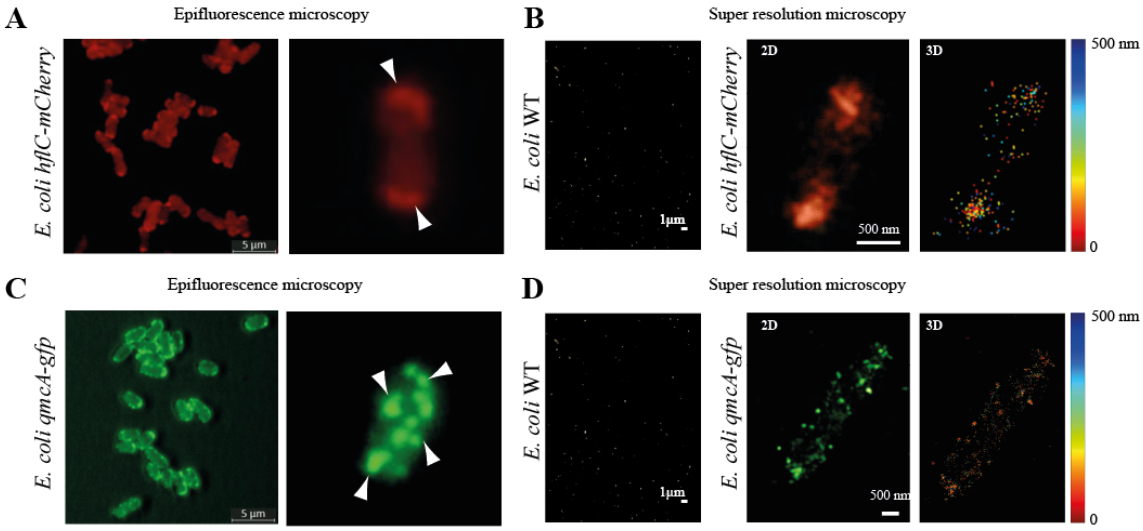

952

953 **Figure 1. Cell localization patterns of HflC and QmcA. A** and **C**: Epifluorescence
954 microscopy of cells expressing HflC-mCherry (A) or QmcA-GFP (C). Arrowheads
955 indicate polar or punctate localization foci. **B** and **D**: Super-resolution microscopy of cells
956 expressing HflC-mCherry (B) or QmcA-GFP (D). *Left panels*: lack of subcellular
957 localization in WT cells. *Center panels*: 3D images-artificial colors (red for HflC-
958 mCherry, green for QmcA-gfp). *Right panels*: 3D localization of HflC-mCherry and
959 QmcA-GFP, with colors corresponding to depth location along the Z axis, 0-500 nm, with
960 0 nm expressed in red, and 500 nm expressed in deep blue. Scales are indicated as white
961 bars.

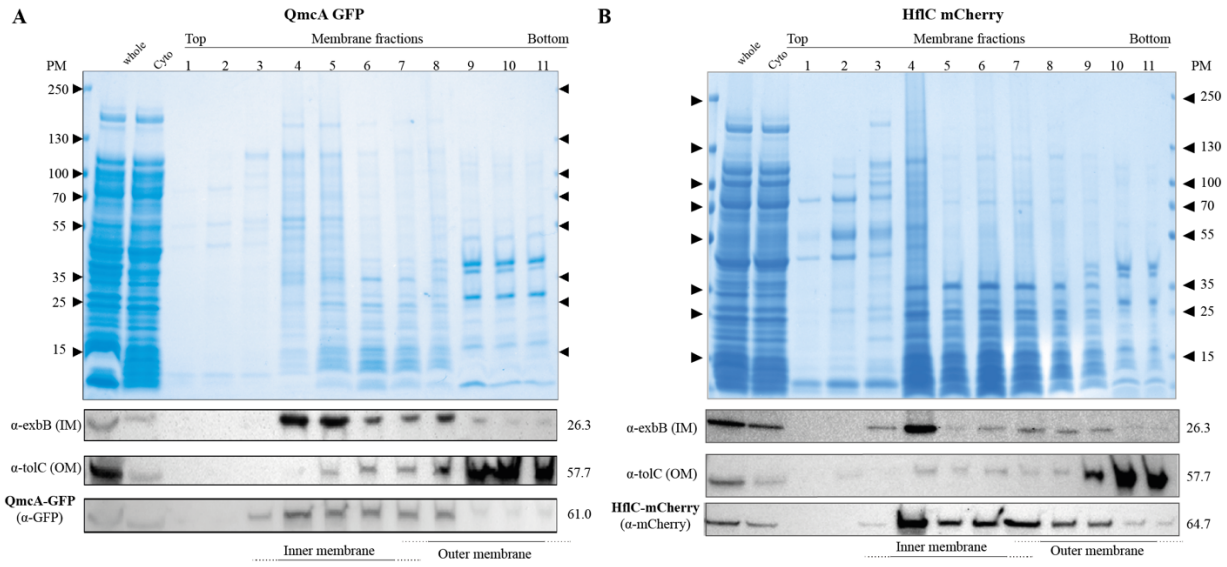

Figure 2. QmcA and HflC localize to the inner membrane. SDS-PAGE and immunodetection analyses of whole-cell extracts, cytosolic fractions, and inner (IM) or outer membrane (OM) fractions prepared from cells expressing QmcA-GFP (**A**) and HflC-mCherry (**B**). Anti-GFP and anti-mCherry antibodies were used to detect the presence of QmcA-GFP and HflC-mCherry, respectively. An anti-ExbB antibody were used to detect the inner membrane- (IM) marker ExbB and anti-TolC antibodies to detect the outer membrane- (OM) marker TolC.

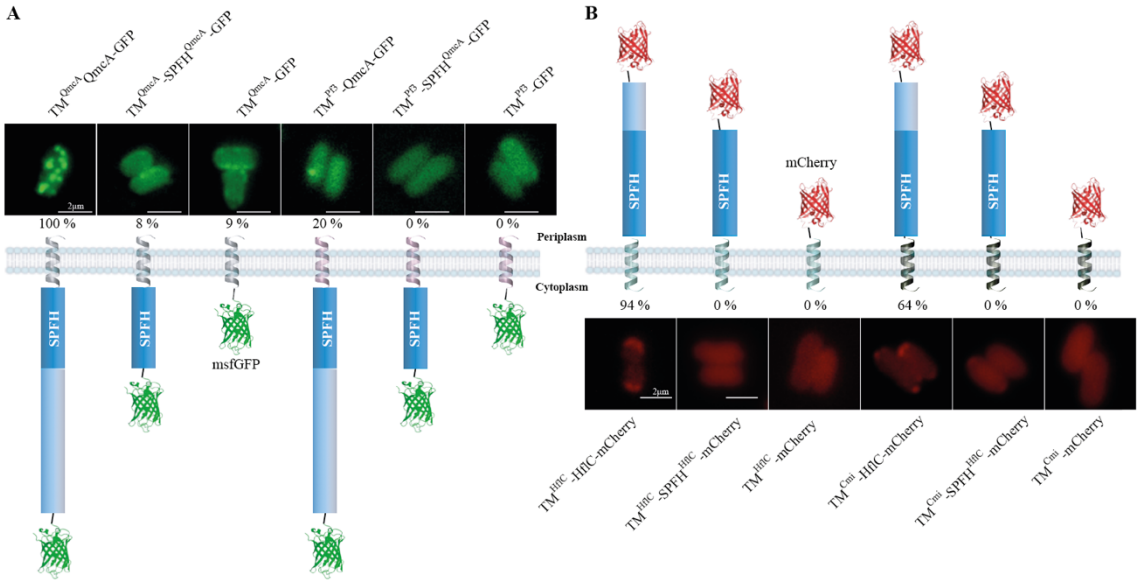

Figure 3. The localization pattern and membrane topology of full-length, domain swapped or truncated versions of QmcA and HflC. (**A**) GFP fusion derivatives of QmcA and (**B**) mCherry fusion derivatives of HflC. The representative images are shown in each strain with the frequencies of cells showing punctate (**A**) or polar localization (**B**). In membrane topology, helical structures represent transmembrane (TM) domains; silver, native TM domain of QmcA; pink, Pf3 domain; green, native TM domain of HflC; black, Cmi domain. Scale bars are 2 µm.

981

982

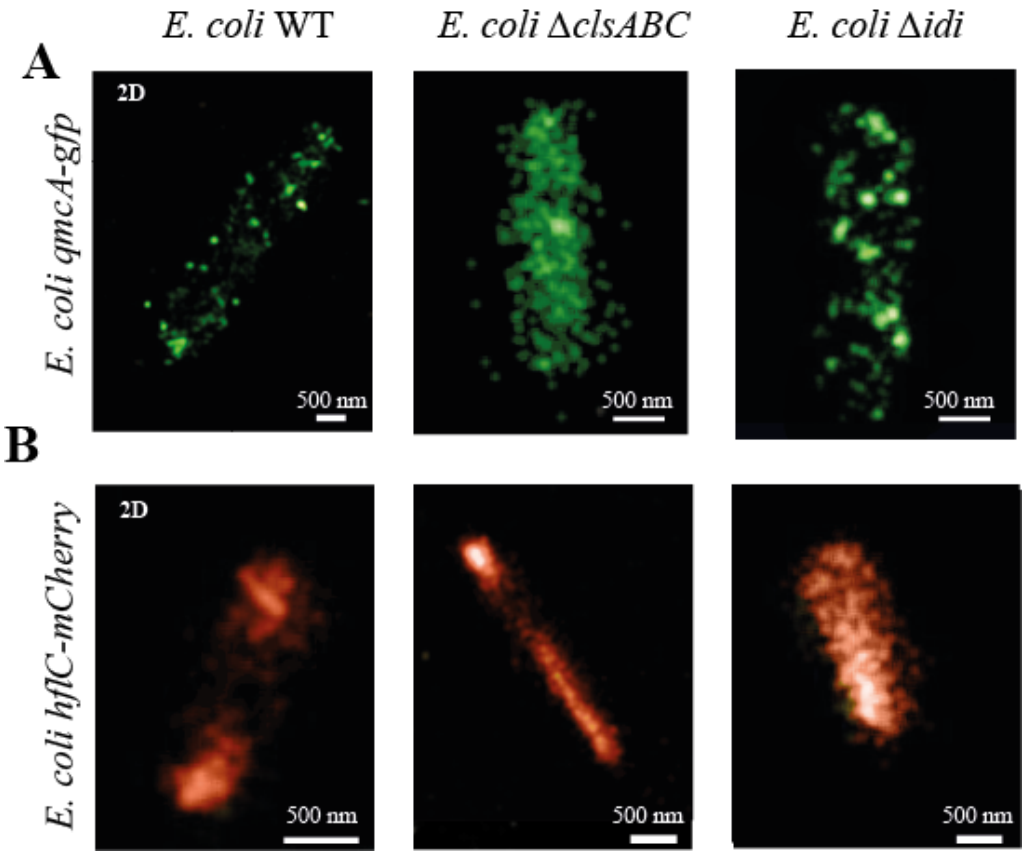

983

984 **Figure 4. Alteration of QmcA and HflC cell localization in *E. coli* cardiolipin and**
985 **isoprenoid pathway mutants.** Two-dimensional super-resolution microscopy images of
986 WT, Δ*clsABC*, and Δ*idi* strains expressing QmcA-GFP (**A**) and HflC-mCherry (**B**) in
987 stationary phase.

988

989

990

991

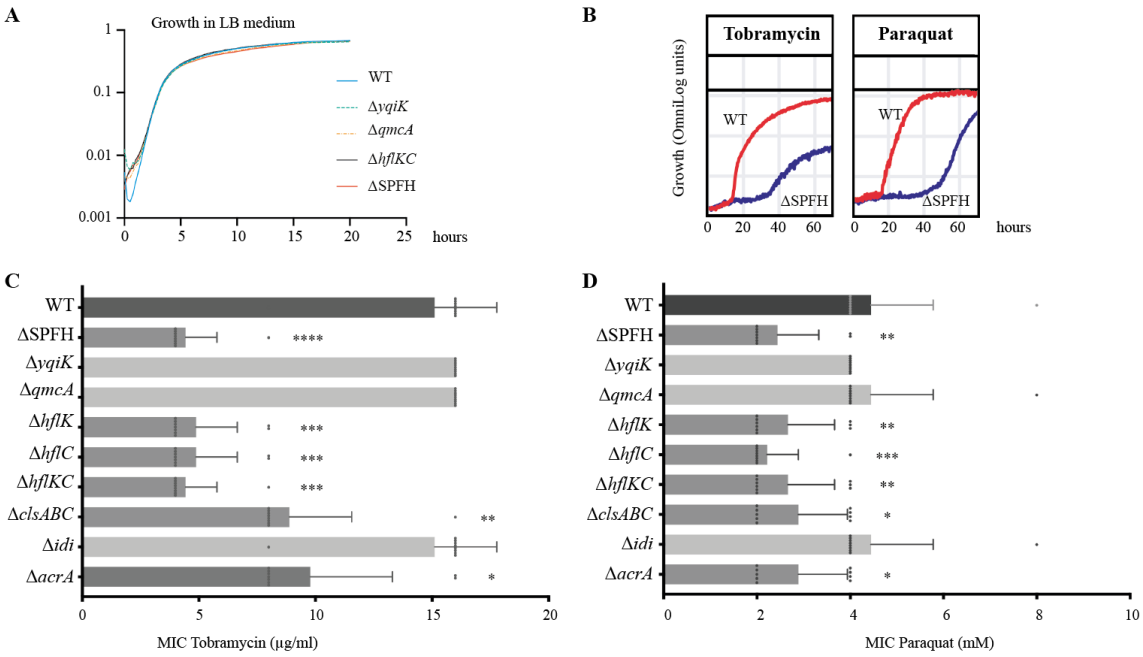

992

993 **Figure 5. Phenotypic analysis of *E. coli* SPFH mutants**. **A**: Bacterial growth curve of
994 WT and SPFH gene deletion mutants in LB medium. **B**: Biolog bacterial growth curve
995 of WT and ΔSPFH in the presence of tobramycin and paraquat. **C**: Minimum inhibitory
996 concentration (MIC) for tobramycin of *E. coli* WT and indicated mutants. **D**: Minimum
997 inhibitory concentration (MIC) for paraquat of *E. coli* WT and indicated mutants. *$p <$
998 0.05, **$p < 0.01$, ***$p < 0.001$, ***$p < 0.0001$ compared with WT.
999
1000

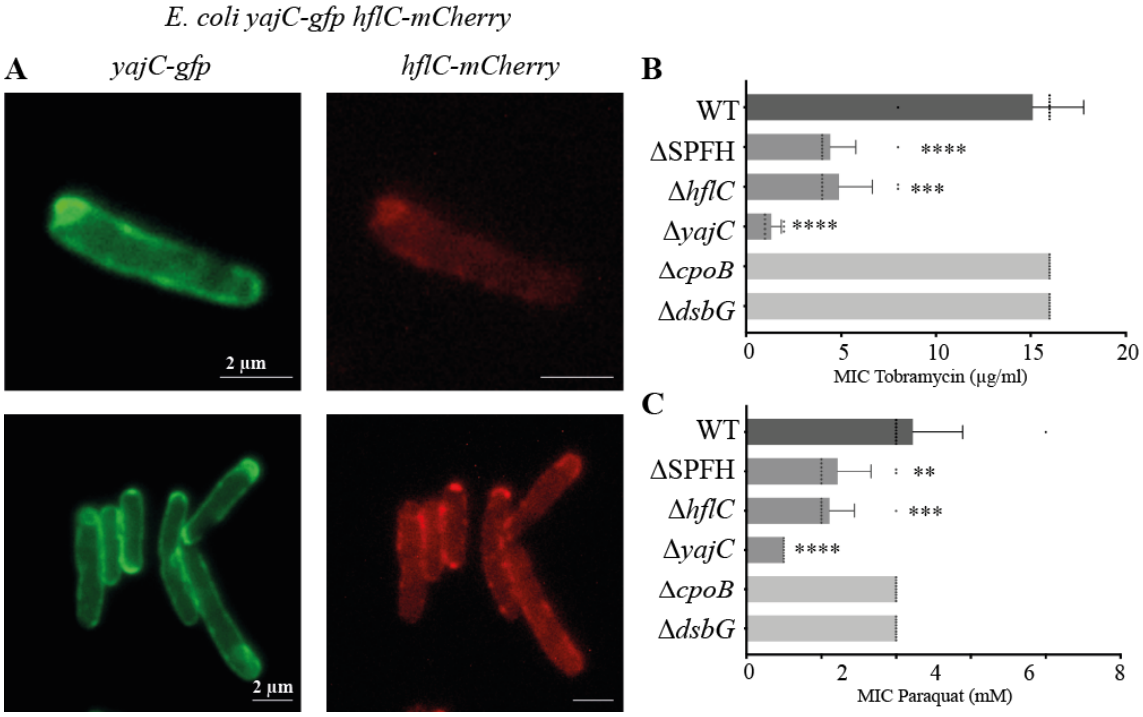

Figure 6. Localization of YajC-GFP and susceptibility of a Δ*yajC* mutant to tobramycin and paraquat. **A:** Epifluorescence microscopic images of cells expressing both YajC-GFP and HflC-mCherry in exponential phase with high and low magnifications. **B** and **C:** Minimum inhibitory concentration (MIC) for tobramycin (B) and paraquat (C) of *E. coli* WT and indicated mutants. WT, *ΔSPFH*, and *ΔhflC* strains are duplicated from Fig. 5C and D and presented here for the comparison. $^{**}p < 0.01$, $^{***}p < 0.001$, $^{****}p < 0.0001$ compared with WT.